A Role for CTCF and Cohesin in Subtelomere Chromatin Organization, TERRA Transcription, and Telomere End Protection

Supplementary Materials

Supplementary Figure Legends

Figure S1. Summary of ChIP-Seq analysis of CTCF, cohesin, and RNAPII binding to type I human subtelomeres. Fragment density profiles were generated for samples and matched IgG controls as described in Methods. The fold enrichment of sample over IgG is shown. The Y axis for each track is auto-scaled to highest peak in each chromosome region shown. Subtelomere identity is indicated in the top left of each panel. (A-D) CTCF_W and SMC1_W were newly generated ChIP-Seq data using human pleural effusion lymphoma cell line BCBL1. CTCF, RNAPII, and Rad21 were derived from human encode data sets using B-lymphoblastoid cell lines. (E) Example enrichment profiles for ChIP-Seq analysis, comparing the standard multi-mapping method used vs allowing only unique mappings. The top track of each dataset pair permitted multi-mapping in the indicated ChIP and control IgG dataset, and the bottom (designated by _U) permitted only unique mappings in both ChIP and IgG control dataset. Binding in the first 15 kb subtelomeres of chromosome arms 10q, 13q, 15q, and XYq are shown.

Figure S2. Summary of ChIP-Seq analysis on type II human subtelomeres. Same as in Figure S1, except for subtelomeres that lack an obvious CTCF binding peak proximal to the terminal repeat tracts.

Figure S3. Validation of CTCF binding site at 10q human subtelomeres in BCBL1 cells. (A) Schematic of the 10q subtelomere showing the relative positions of the 29 bp repeat element, CpG island, and TTAGGG terminal repeats. (B) ChIP-qPCR for TRF1, TRF2, CTCF, RNAPII, Rad21, and SMC1 relative to IgG controls using primers for the 10q subtelomere at positions close (~400 bp) to TTAGGG repeat (black), at CpG island (red), or ~2 kb from terminal repeats (green). Bar graph represents the average value of percentage of input for each ChIP from three independent PCR (Mean ± SD).

Figure S4. Chromatin organization of 10q subtelomeres. (A-B) Conventional ChIP-qPCR was used to assay CTCF, Rad21, SMC3, TRF1, TRF2, histone H3K4me2 and me3, H3K9me2 and me3, and RNAPII binding at various nucleotide positions relative to the TTAGGG repeat tract (position 0) in the 10q subtelomere or control *Gapdh* region for either U2OS (A) or HCT116 (B) cell lines. Bar graph represents the average value of percentage of input for each ChIP from three independent ChIP experiments (Mean ± SD).

Figure S5. Additional examples for chromatin organization of type I subtelomeres. (A) Conventional ChIP-qPCR was used to assay CTCF, Rad21, SCM3, TRF1, TRF2, histone H3K4me2 and me3, H3K9me2 and me3, RNAPII, and control IgG binding at various nucleotide positions relative to the TTAGGG repeat tract (position 0) in the 13q subtelomere for U2OS cell line. Bar graph represents the average value of percentage of input for each ChIP from three independent ChIP experiments (Mean ± SD). (B) Same as in the panel A, except that 15q subtelomere was analyzed by ChIP-qPCR.

Figure S6. CTCF depletion reduces TERRA levels in HCT116 cells. (A) Northern blot analysis of TERRA in HCT116 cells transfected with siControl, siCTCF-1, or siCTCF-2 with control 18S (middle panel). EtBr staining of the gel (lower panel) indicates RNA integrity (28S and 18S bands). About 10 μg of total RNA isolated from transfected cells at 4 days post-transfection was loaded in each lane. Numbers at the bottom show the average value of TERRA signals relative to 18S RNA signals in siCTCF versus siControl from three independent experiments. (B) Western blot of HCT116 cells transfected with siRNA control, siCTCF-1, or siCTCF-2 and assayed with anti-CTCF or anti-Actin. (C) qRT-PCR of TERRA from individual telomeres in HCT cells transfected with siControl, siCTCF-1, or siCTCF-2 at 4 days post-transfection. Relative RT-PCR represents the value calculated by ΔΔCT methods relative to siControl and *Gapdh*. Bar graph represents the average value from three independent PCR reactions (Mean ± SD).

Figure S7. TERRA transcribed from type II subtelomeres are less responsive to CTCF depletion. (A) Additional examples of Northern blot analysis of TERRA used for quantification in Fig. 4F. EtBr staining of the gel (lower panel) indicates RNA integrity (28S and 18S bands). Equal amount of total RNA (~7.5 μg) isolated from cells at 4 days post-transfection was loaded in each lane. (B) qRT-PCR of TERRA from type I telomeres at 10q, XYq, 2q, and 17p in U2OS cells treated with siControl, siCTCF-1, and siCTCF-2. qRT-PCR of CTCF was used as control for CTCF depletion by CTCF siRNAs. Relative RT-PCR represents the value calculated by ΔΔCT methods relative to siControl and *Gapdh*. Bar graph represents the average value from three independent

CTCF depletion experiments (Mean ± SD). (C) The same as in B, except that TERRA derived from type II telomeres at 3p, 7p, XYp, and 12q was assayed by qRT-PCR.

Figure S8. Effect of shRNA depletion of Rad21 and CTCF on TERRA expression. (A) Western blot of U2OS cells transduced with shControl, shCTCF, or shRad21, and assayed for expression levels of CTCF, Rad21, SMC3, TRF1, and Actin at 6 days post lentiviral infection. (B) Additional examples of Northern blot analysis of TERRA used for quantification in Fig. 5C. EtBr staining of the gel (lower panel) indicates RNA integrity (28S and 18S bands).

Figure S9. shRNA depletion of Rad21 and CTCF reduces TERRA expression in HCT116 cells. (A) Western blot of HCT cells transduced with shControl, shCTCF, or shRad21, and assayed for expression levels of CTCF, Rad21, TRF1, and Actin at 6 days post-lentiviral infection. (B) qRT-PCR of TERRA from individual telomeres at 10q, XYq, 13q, 15q, 16p, and 7p together with CTCF and Rad21 expression in infected cells as above. Relative RT-PCR represents the value calculated by ΔΔCT methods relative to shControl and *Gapdh*. Bar graph represents the average value from three independent PCR reactions (Mean ± SD).

Figure S10. CTCF and Rad21 depletion leads to a loss of RNAPII and TRF binding at 10q subtelomeres. (A) ChIP-qPCR for CTCF, Rad21, and SMC3 were shown at various positions of the 10q subtelomere relative to the TTAGGG repeat tracts (position 0). U2OS cells were transduced with shControl (black), shCTCF (red), or shRad21

(green) and assayed by ChIP at day 6 post-infection. ChIP-qPCR at *Gapdh* region was included as a control for specificity. Bar graph represents the average value of % input for each ChIP from three independent experiments (Mean ± SD). (B-D) Same as in A, except that TRF1, TRF2, or control IgG (B), RNAPII or RNAPII S2 (C), or histone H3 K4 or K9 tri-methylation (D) were assayed by ChIP-qPCR in infected U2OS cells.

Figure S11. Effect of multiple CTCF shRNAs on TRF binding at 10q subtelomeres. **(**A) Western blot of U2OS cells transduced with lentiviruses for CTCF or control, and assayed for expression levels of CTCF and Actin at 6 days post-lentiviral infection. (B-F) ChIP-qPCR for IgG (B), CTCF (C), SMC3 (D), TRF1 (E), and TRF2 (F) were shown at various positions of the 10q subtelomere relative to the TTAGGG repeat tracts (position 0). U2OS cells were transduced with shControl (black), shCTCF-2, or shCTCF-5 and assayed by ChIP at day 6 post-infection. Bar graph represents the average value of % input for each ChIP from three qPCR reactions (Mean ± SD).

Figure S12. MNase I digestion of chromatin at telomeres and subtelomeres after CTCF and Rad21 depletion. (A) Micrococcal nuclease (MNase) pattern assay was performed in U2OS cells transfected with siControl, siCTCF-1, or siCTCF-2 for 4 days. Nuclei was treated with indicated units of MNase, fractionated on 1.2% agarose gel, and assayed by hybridization with either ^{32}P-labeled $(TAACCC)_4$ probe (left panel) or ^{32}P-labeled Alu probe (right panel). (B) MNase pattern assay was performed in U2OS cells transduced with shControl, shCTCF-5, or shRad21 for 6 days. Nuclei was treated with indicated units of MNase, and assayed by hybridization with either ^{32}P-labeled XYq probe (left panel) or ^{32}P-labeled $(TAACCC)_4$ probe (right panel).

Figure S13. CTCF depletion by siRNA leads to an increase in telomere associated DNA damage foci (TIFs). (A) U2OS cells were transfected with siControl, siCTCF-1, or siCTCF-2 for 4 days and assayed by immunofluorescence (IF) with antibody to TRF2 (red) and antibody to 53BP1 (green). Dapi (blue) and merge image is shown to the right. (B) Quantification of the percentage of cells with more than five TIFs as represented in panel A. The bar graph is the mean and SDs derived from quantification of more than 100 nuclei from three independent TIF assays. p value was calculated by two-tailed Student's t –Test. (C) IF with anti-TRF2 (red) or γH2AX (green) in U2OS cells transfected with siControl, siCTCF-1, or siCTCF-2 for 4 days. Dapi (blue) and merge image is shown to the right. (D) Quantification of telomere associated DNA damage foci as represented in panel C. The bar graph is the mean and SDs derived from quantification of more than 100 nuclei from three independent TIF assays. p value was calculated by two-tailed Student's t –Test.

Figure S14. Telomere repeat length does not change in CTCF and Rad21 depleted cells. (A) Telomere repeat length was measured by restriction digest with *Alu*I/*Mbo*I and Southern hybridization with TTAGGG-specific probe in U2OS and HCT166 cells transfected with siCon or siCTCF-specific siRNA at 4 days post-transfection. The same blot was stripped, and hybridized with Alu-specific probe shown in right panel. (B) Telomere repeat length of HCT116 cells infected with shControl, shCTCF-5, or shRad21 was assayed at 6 or 10 days post-infection by Southern blotting using ^{32}P-$(TAACCC)_4$ probe. Ethidium bromide staining of total DNA digest was used as a control for DNA

loading (left panel). (C) Telomere repeat length of U2OS cells infected with shControl, shCTCF-5, or shRad21 at 4, 6 or 10 days post-infection. Genomic DNA was digested with *Alu*I/*Mbo*I, fractionated by pulsed-field gel electrophoresis, and hybridized with ^{32}P-$(TAACCC)_4$ probe for telomere repeats (right panel). Ethidium bromide staining of total DNA digest was used as a control for DNA loading (left panel). Numbers on the left show the position of DNA markers in Kb.

Figure S15. Melting curve control for primers used in ChIP-qPCR. (A-D) Example snapshots of dissociation curves of ChIP-qPCR primers for XYq (A), 10q (B), 13q (C), 15q (D) subtelomeres. All of these primers show single amplicon peak.

Figure S16. Melting curve control for primers used in qRT-PCR analysis of TERRA RNA. (A) Example snapshots of dissociation curves of qRT-PCR primers for TERRA RNA derived from type I subtelomeres. (B) Example snapshots of dissociation curves of qRT-PCR primers for TERRA RNA derived from type II subtelomeres.

Supplementary File 1. DNA sequences of human subtelomere assemblies (1-15K) in concatenated FASTA format.

Supplementary File 2. Comparison of ChIP-Seq reads by unique mapping and multi mapping. (A) ChIP-Seq dataset characteristics. Read mapping statistics for each dataset used, both genome-wide and just for the 15 K subtelomere assemblies. (B) 15K Subtel Mappings. Read mapping statistics broken down by each 15K Subtel Region for

the CTCF (public), CTCF_W (Wistar), RNAPII (public), SMC1_W (Wistar), and Rad21 (public) datasets and their respective controls. (C) Distal peak region mappings. Read mapping statistics broken down by the distal peak-containing segments of each subtel region for the CTCF (public), CTCF_W (Wistar), RNAPII (public), SMC1_W (Wistar), and Rad21 (public) datasets and their respective controls. (D) 29-mer VNTR multi mappings. Read mapping statistics for the 29-mer VNTR segments of 10q, XYq, 13q, and 15q.

Supplementary Table S1. List of primers used for quantitative RT-PCR, and copy number/ known loci amplified by subterminal TERRA primer sets. Subterminal Sequence Families are as defined previously (Riethman, 2008), and the number of distinct genomic loci matching the primer set computationally is given in parentheses. The genomic locations of each of these loci are indicated; "Tel" indicates immediately adjacent to the telomere repeat tract in the sequence organization shown in Figures 1 and 2. "Trunc" indicates that while the assay is derived from the indicated telomere-adjacent sequence from a specific allele, other alleles and subtelomeric locations of the amplicon are within duplicated subtelomeric DNA but not immediately adjacent to the terminal (TTAGGG)n tracts ("Subtel"). The number of non-subtelomeric duplicated sites, where they exist for an assay, are as indicated.

Transcript	Primer	Sequence (5' -3')	Subterm Family (Number of Copies with amplicon match)	Known Loci	Other Comments
CTCF	5'primer	GACCCCACCCTTCTTCAGATG	na	na	
CTCF	3'primer	CCACAGCAGCCTCTGCTTCT	na	na	
Rad21	5'primer	GGCCAGCAGAACAAACATAGATG	na	na	
Rad21	3'primer	TTTGTCCAGCTTTTCGCTTAACT	na	na	
10q-TERRA	5'primer	GCCTTGCCTTGGGAGAATCT	D (10)	1q,2q,4q,5q,6q, 10q,13q, 16q, 21q,22q (Tel)	
10q-TERRA	3'primer	AAAGCGGGAAACGAAAAGC			
XYq-TERRA	5'primer	CCCCTTGCCTTGGGAGAA	C (3)	9p, 19p, XYq (Tel)	
XYq-TERRA	3'primer	GAAAGCAAAAGCCCCTCTGA			
2q-TERRA	5'primer	GCCTTGCCTTGGGAGAATCT	D (10)	1q,2q,4q,5q,6q, 10q, 13q, 16q, 21q,22q (Tel)	
2q-TERRA	3'primer	AAAGCGGGAAACGAAAAGC			
13q-TERRA	5'primer	GCACTTGAACCCTGCAATACAG	D (10)	1q,2q,4q,5q,6q, 10q,13q, 16q, 21q,22q (Tel)	
13q-TERRA	3'primer	CCTGCGCACCGAGATTCT			

15q-TERRA	5’primer	TGCAACCGGGAAAGATTTTATT	C (2)	15q, 19p (Tel)	
15q-TERRA	3’primer	GCGTGGCTTTGGGACAACT			
16p-TERRA	5’primer	TGCAACCGGGAAAGATTTTATT	C (3)	9p,16p,19p (Tel)	
16p-TERRA	3’primer	GCCTGGCTTTGGGACAACT			
7p-TERRA	5’primer	GGAGGCTGAGGCAGGAGAA	Trunc (13)	7p (Tel); 1p, 3q, 9q, 11p, 16q,19p (Subtel); + 6 internal dup sites	
7p-TERRA	3’primer	CAATCTCGGCTCACCACAATC			
3p-TERRA	5’ primer	ACGACGTCTACTTTGTTCCTTGGT	1	3p (Tel)	
3p-TERRA	3’ primer	AAGAGCACACGGCCAGACA			
XYp-TERRA	5’ primer	CCACAACCCCACCAGAAAGA	1	XYp	
XYp-TERRA	3’ primer	GCGCGTCCGGAGTTTG			
12q-TERRA	5’ primer	ATTTCCCGTTTTCCACACTGA	2	7q, 12q (Tel)	
12q-TERRA	3’ primer	CTGTTTGCAGCGCTGAATATTC			
17p-TERRA	5’ primer	GGGACAGAAGTGGATAAGCTGATC	Trunc (7)	17p (Tel); 1p, 3q, 7p, 9q, 11p,16q (Subtel)	
17p-TERRA	3’ primer	GATCCCACTGTTTTTATTACTGTTCCT			
17q-TERRA	5’primer	AGCTACCTCTCTCAACACCAAGAAG	B, D (13)	2q,4q,5q,6p,6q, 8p,10q,16q,17q,19p,19q,21q,22q (Tel)	
17q-TERRA	3’primer	GTCCATGCATTCTCCATTGATAAG			
Gapdh	5’primer	AGCCACATCGCTCAGACAC	na	na	
Gapdh	3’primer	GCCCAATACGACCAAATCC			

Supplementary Table S2. List of primers used for ChIP, and copy number/ known loci amplified by ChIP primer sets. Subterminal Sequence Families are as defined previously (Riethman, 2008), and the number of distinct genomic loci matching the primer set computationally is given in parentheses. The genomic locations of each of these loci are indicated; "Tel" indicates immediately adjacent to the telomere repeat tract in the sequence organization shown in Figures 1 and 2. "2qfus" refers to the evolutionarily recent fusion junction of primate telomeres to form modern human chromosome 2; this locus retains similarity to subterminal family C on one side of the fusion junction, and family D on the other side. No non-telomeric sites except for the 2qfus site (where indicated) are amplified by the ChIP-seq primers used.

Region	Primer	Sequence (5' -3')	Subterm Family (Number of Copies with amplicon match)	Known Loci	Other Comments
XYq-1/ -109	5'primer	CCCCTTGCCTTGGGAGAA	C (3)	9p, 19p, XYq (Tel)	
XYq-1/ -109	3'primer	GAAAGCAAAAGCCCCTCTGA			
XYq-3/ -2733	5'primer	CCAAGGCCTGGCAGAGTCT	C (7)	9p,12p,15q,16p,19p, XYq (Tel); 2qfus (internal)	
XYq-3/ -2733	3'primer	TGCGGACTGTTTGCTGCTT			
XYq-2/-966	5'primer	GGTGGAACTTCAGTAATCCGAAA	C (5)	9p,15q,16p,19p,XYq (Tel)	
XYq-2/-966	3'primer	AGCAAGCGGGTCCTGTAGTG			
XYq-1299	5'primer	ATTATAGGGAAACACCAGGAGCAT	C (6)	9p,15q,16p,19p,XYq (Tel); 2qfus (internal)	
XYq-1299	3'primer	TACTTTTAAACCCAGGAATCCCATA			
XYq-1456	5'primer	GTGCCTGTTTCTCCACAAAGTGT	C (7)	9p,12p,15q,16p,19p, XYq (Tel); 2qfus (internal)	

XYq-1456	3'primer	ATCTCCAGGGCTTCACCTGTT			
XYq-1742	5'primer	TCTGTTCATGTGTATTTGCTGTCTCT	C (7)	9p,12p,15q,16p,19p, XYq (Tel); 2qfus (internal)	
XYq-1742	3'primer	AAAGGCCTGGTGGAAAGGA			
13q-152	5'primer	GCACTTGAACCCTGCAATACAG	D (10)	1q, 2q, 4q, 5q, 6q, 10q, 13q, 16q, 21q, 22q (Tel)	
13q-152	3'primer	CCTGCGCACCGAGATTCT			
13q-957 CTCF site	5'primer	AGTGGAACCTGAGTATTCTGAAAAGC	D (11)	1q, 2q, 4q, 5q, 6q, 10q, 13q, 16q, 19q, 21q, (Tel); 2qfus (internal)	
13q-957 CTCF site	3'primer	GCAGTTGTCCTACTCGCCAGTA			
13q-6545	5'primer	TCCCTCCCACGACATTTAGG	B, D (14)	1q,2q,4q,5q,6q,10q, 13q,16q, 17q, 19p, 19q,21q,22q (Tel); 2qfus (internal)	RPL23a pseudogene copies
13q-6545	3'primer	CCTGTTTCCCCACCCAGAT			
15q-265	5'primer	TGCAACCGGGAAAGATTTTATT	C (2)	15q, 19p (Tel)	
15q-265	3'primer	GCGTGGCTTTGGGACAACT			
15q-941 CTCF site	5'primer	TGCACGCGCAGAAACTCA	C (3)	15q, 16p, 19p (Tel)	
15q-941 CTCF site	3'primer	CCGGCTTTTCGGATTACTGA			
15q-6700	5'primer	CAGAACCCAGCTCACCTACCTT	C (7)	9p,12p,15q,16p,19p, XYq (tel); 2qfus (internal)	WASH gene copies
15q-6700	3'primer	AACTGCCCACCTTCCACACT			
10q-1/-396	5'primer	GCCTTGCCTTGGGAGAATCT	D (10)	1q, 2q, 4q, 5q, 6q, 10q, 13q, 16q, 21q, 22q (Tel)	
10q-1/-396	3'primer	AAAGCGGGAAACGAAAAGC			
10q-2/-1122	5'primer	CAGAGACGAGTGGAACCTGAGTAAT	B, D (14)	1q,2q,4q,5q,6q,8p, 10q,13q,16q,19p,19q, 21q,22q (Tel); 2qfus (internal)	

10q-2/-1122	3’primer	TGGGCAAGCTGGTCCTGTAG			
10q-1539	5’primer	CGCCTCCTGCACCACTTAAA	B, D (14)	1q,2q,4q,5q,6q,8p, 10q,13q,16q,19p,19q, 21q,22q (Tel); 2qfus (internal)	
10q-1539	3’primer	CGCAGTAATAGCTCCTTTTCAG TTT			
10q-3/-1997	5’primer	GCTGACAGCGGTCACGTTT	B, D (14)	1q,2q,4q,5q,6q,8p, 10q,13q,16q,19p,19q, 21q,22q (Tel); 2qfus (internal)	
10q-3/-1997	3’primer	TAGGGCAGAGAAAGACATTCA AAA			
GAPDH	5’primer	TGGGCTACACTGAGCACCAG			
GAPDH	3’primer	GGGTGTCGCTGTTGAAGTCA			

Supplementary Table S3. List of probes used for EMSA and Fluorescence Polarization (FP) Assay. Point mutations on CTCF binding sites were shown in red.

Probe	Sequence (5'-3')
XYq-5'	GATCCTGCTGTGCCAGGGCGCCCCCTGCTGGCGACTAGGGCAACTA
XYq-3'	AGCTTAGTTGCCCTAGTCGCCAGCAGGGGGCGCCCTGGCACAGCAG
10q-5'	GATCCAGCCCGTTTCGGGCGCCCCCTGCTTGCAGCCGGGCACTACA
10q-3'	AGCTTGTAGTGCCCGGCTGCAAGCAGGGGGCGCCCGAAACGGGCTG
7p-5'	GATCCGGGCGGGATCGCGCGCCCTCTGGTGGCGCCATGGTTCAGCA
7p-3'	AGCTTGCTGAACCATGGCGCCACCAGAGGGCGCGCGATCCCGCCCG
ΔXYq -5'	GATCCTGCTGTGCCAGAATACAAAATGCTAATAACTAGGGCAACTA
ΔXYq -3'	AGCTTAGTTGCCCTAGTTATTAGCATTTTGTATTCTGGCACAGCAG
Δ10q -5'	GATCCAGCCCGTTTCGAATACAAAATGCTTAAAACCGGGCACTACA
Δ10q -3'	AGCTTGTAGTGCCCGGTTTTAAGCATTTTGTATTCGAAACGGGCTG
Δ7p -5'	GATCCGGGCGGGATCATATATTTTCTAGTAATATCATGGTTCAGCA
Δ7p -3'	AGCTTGCTGAACCATGATATTACTAGAAAATATATGATCCCGCCCG

Fig. S1A

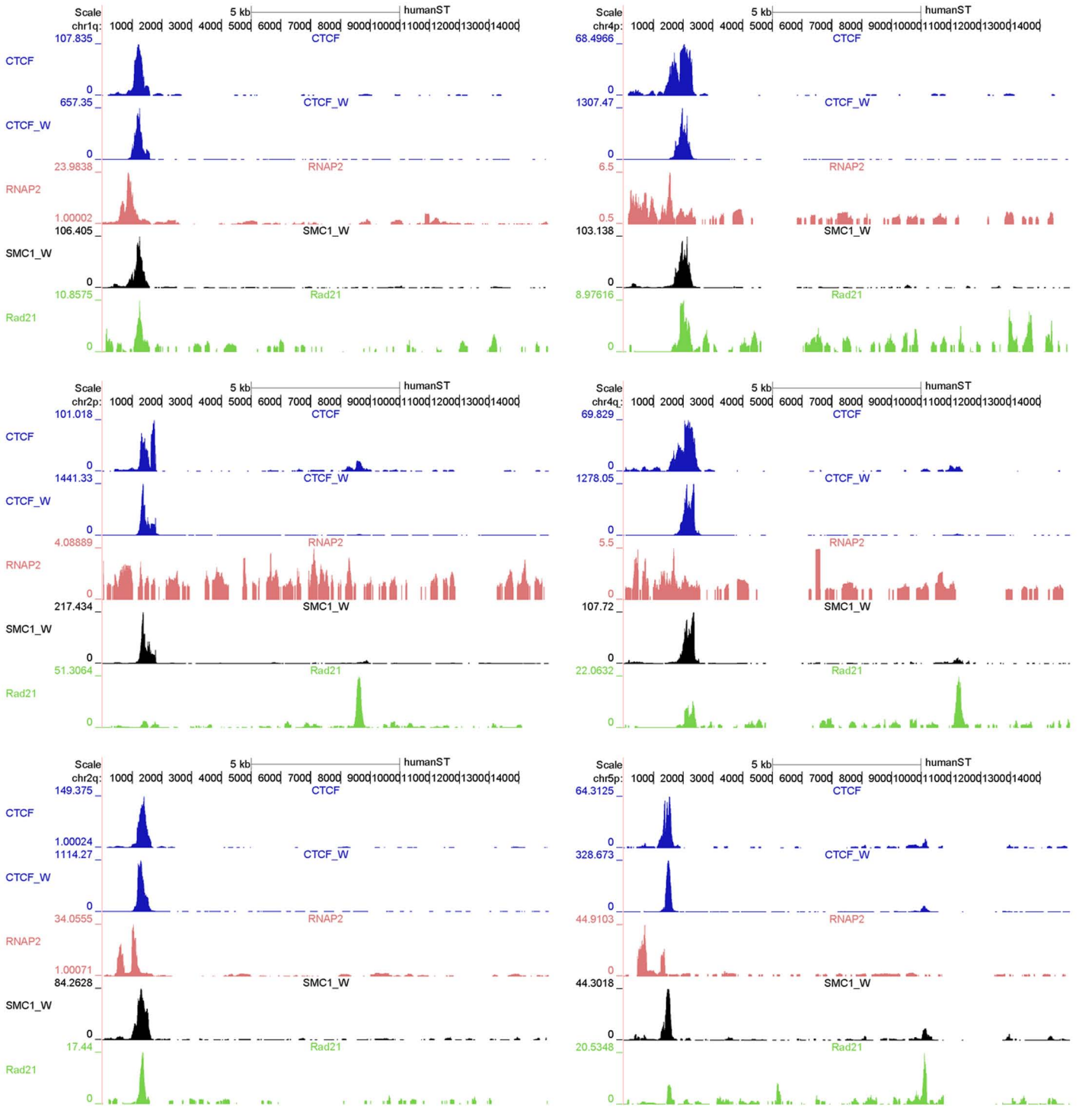
Scale
chr1q:
5 kb
humanST
1000 2000 3000 4000 5000 6000 7000 8000 9000 10000 11000 12000 13000 14000
107.835
CTCF
CTCF
0
657.35
CTCF_W
CTCF_W
0
23.9838
RNAP2
RNAP2
1.00002
106.405
SMC1_W
SMC1_W
0
10.8575
Rad21
Rad21
0
Scale
chr4p:
5 kb
humanST
1000 2000 3000 4000 5000 6000 7000 8000 9000 10000 11000 12000 13000 14000
68.4966
CTCF
0
1307.47
CTCF_W
0
6.5
RNAP2
0.5
103.138
SMC1_W
0
8.97616
Rad21
0
Scale
chr2p:
5 kb
humanST
1000 2000 3000 4000 5000 6000 7000 8000 9000 10000 11000 12000 13000 14000
101.018
CTCF
CTCF
0
1441.33
CTCF_W
CTCF_W
0
4.08889
RNAP2
RNAP2
0
217.434
SMC1_W
SMC1_W
0
51.3064
Rad21
Rad21
0
Scale
chr4q:
5 kb
humanST
1000 2000 3000 4000 5000 6000 7000 8000 9000 10000 11000 12000 13000 14000
69.829
CTCF
0
1278.05
CTCF_W
0
5.5
RNAP2
0
107.72
SMC1_W
0
22.0632
Rad21
0
Scale
chr2q:
5 kb
humanST
1000 2000 3000 4000 5000 6000 7000 8000 9000 10000 11000 12000 13000 14000
149.375
CTCF
CTCF
1.00024
1114.27
CTCF_W
CTCF_W
0
34.0555
RNAP2
RNAP2
1.00071
84.2628
SMC1_W
SMC1_W
0
17.44
Rad21
Rad21
0
Scale
chr5p:
5 kb
humanST
1000 2000 3000 4000 5000 6000 7000 8000 9000 10000 11000 12000 13000 14000
64.3125
CTCF
0
328.673
CTCF_W
0
44.9103
RNAP2
0
44.3018
SMC1_W
0
20.5348
Rad21
0

Fig. S1B

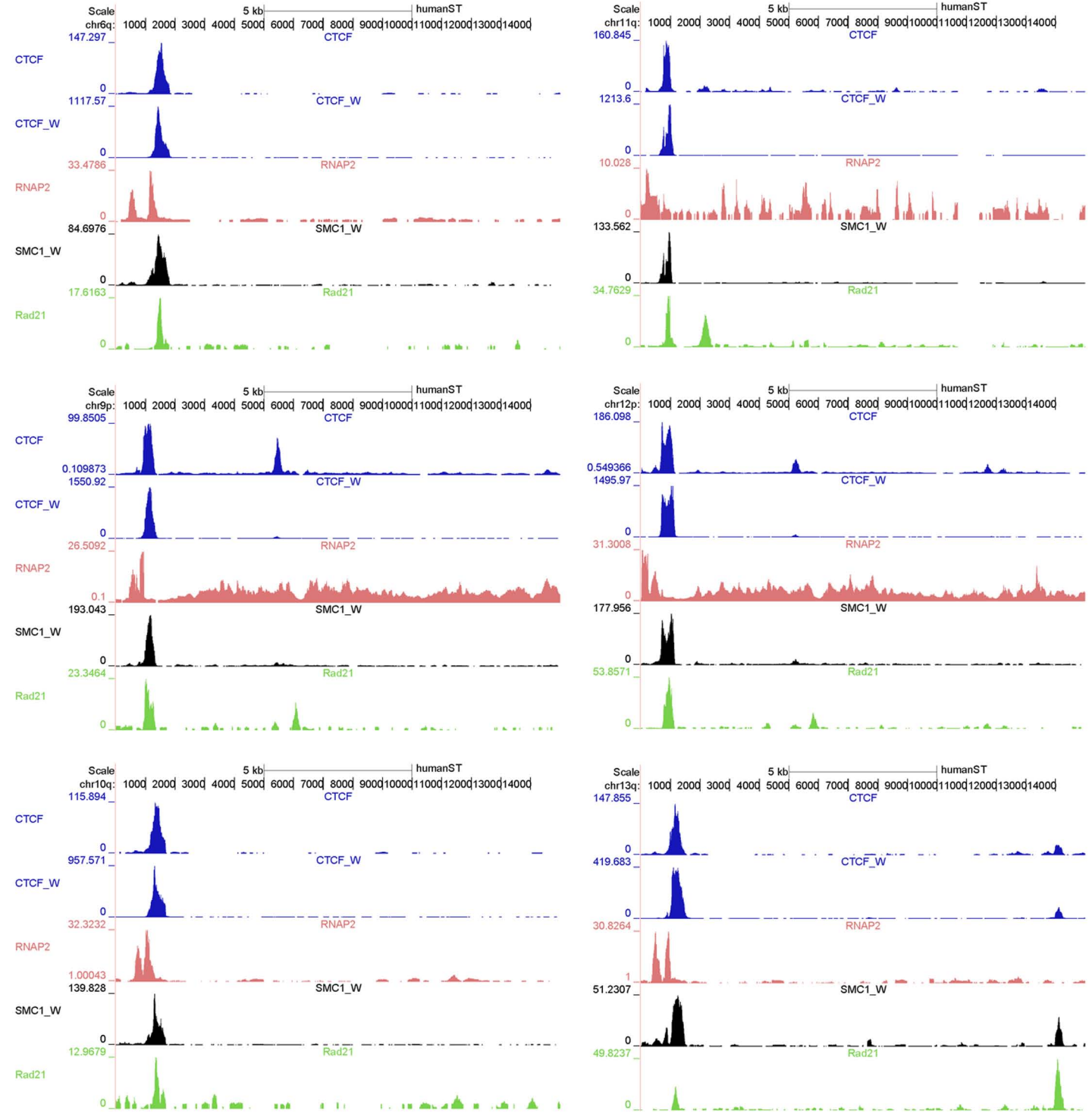
Scale
5 kb
humanST
chr6q:
100[200[300[400[500[600[700[800[900[1000[1100[1200[1300[1400[
CTCF
CTCF_W
RNAP2
SMC1_W
Rad21
chr11q:
chr9p:
chr12p:
chr10q:
chr13q:

Fig. S1C


Scale
5 kb
humanST
chr14q:
chr17p:
chr15q:
chr18p:
chr16p:
chr18q:
1000 2000 3000 4000 5000 6000 7000 8000 9000 10000 11000 12000 13000 14000
CTCF
CTCF_W
RNAP2
SMC1_W
Rad21
177.353
980.702
69.1236
103.341
110.473
159.283
1291.68
2.41494
251.506
38.4528
164.247
1.01372
1743.26
20.9074
1.00858
182.187
40.595
45.3477
70.7261
234.669
172.439
7.92142
162.281
1200.08
36.0744
166.544
46.7012
94.8882
279.671
8.01982
132.01
72.8316

Fig. S1D

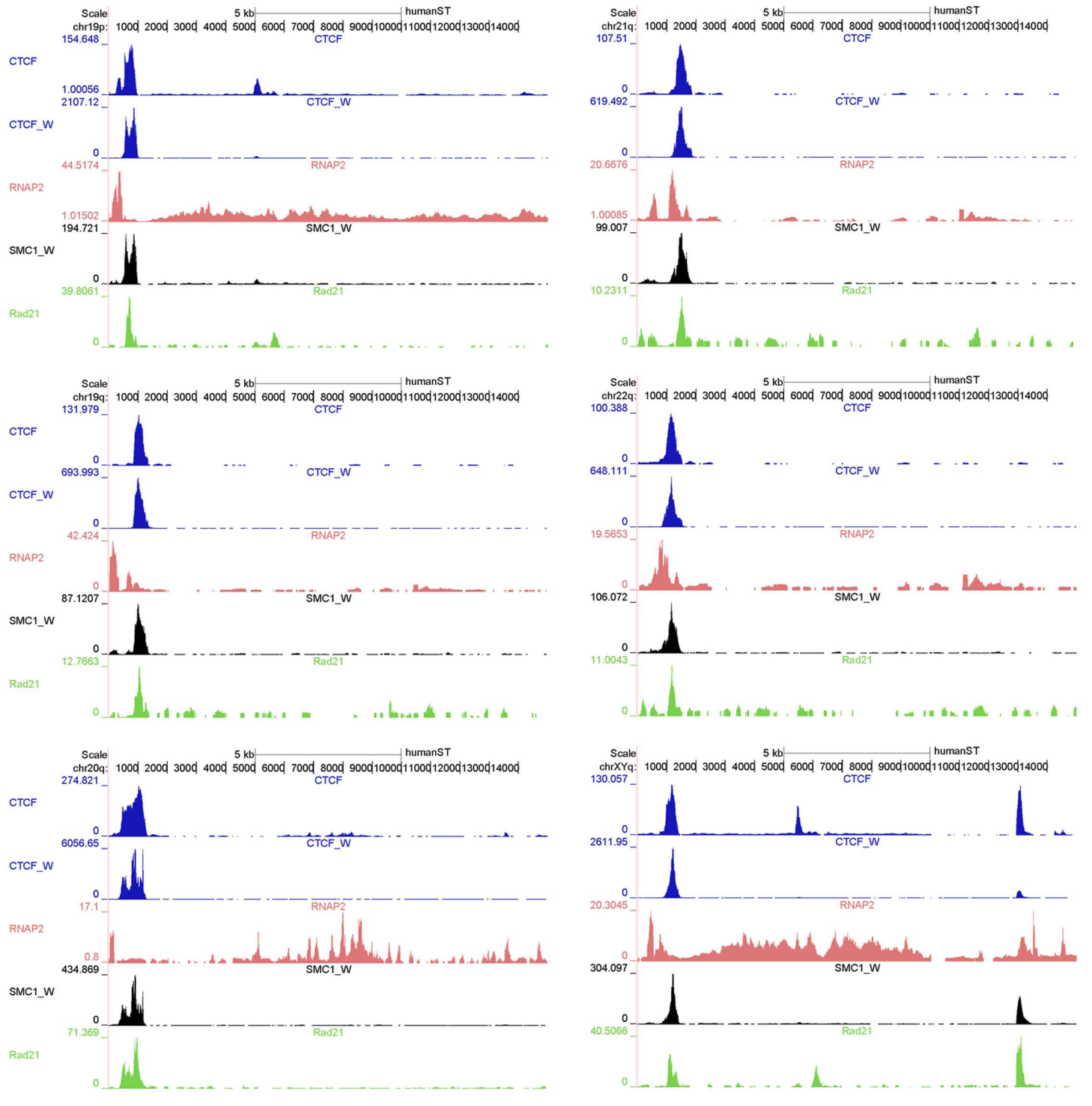
Scale
5 kb
humanST
chr19p:
chr21q:
chr19q:
chr22q:
chr20q:
chrXYq:
1000 2000 3000 4000 5000 6000 7000 8000 9000 10000 11000 12000 13000 14000
CTCF
CTCF_W
RNAP2
SMC1_W
Rad21

Fig. S1E

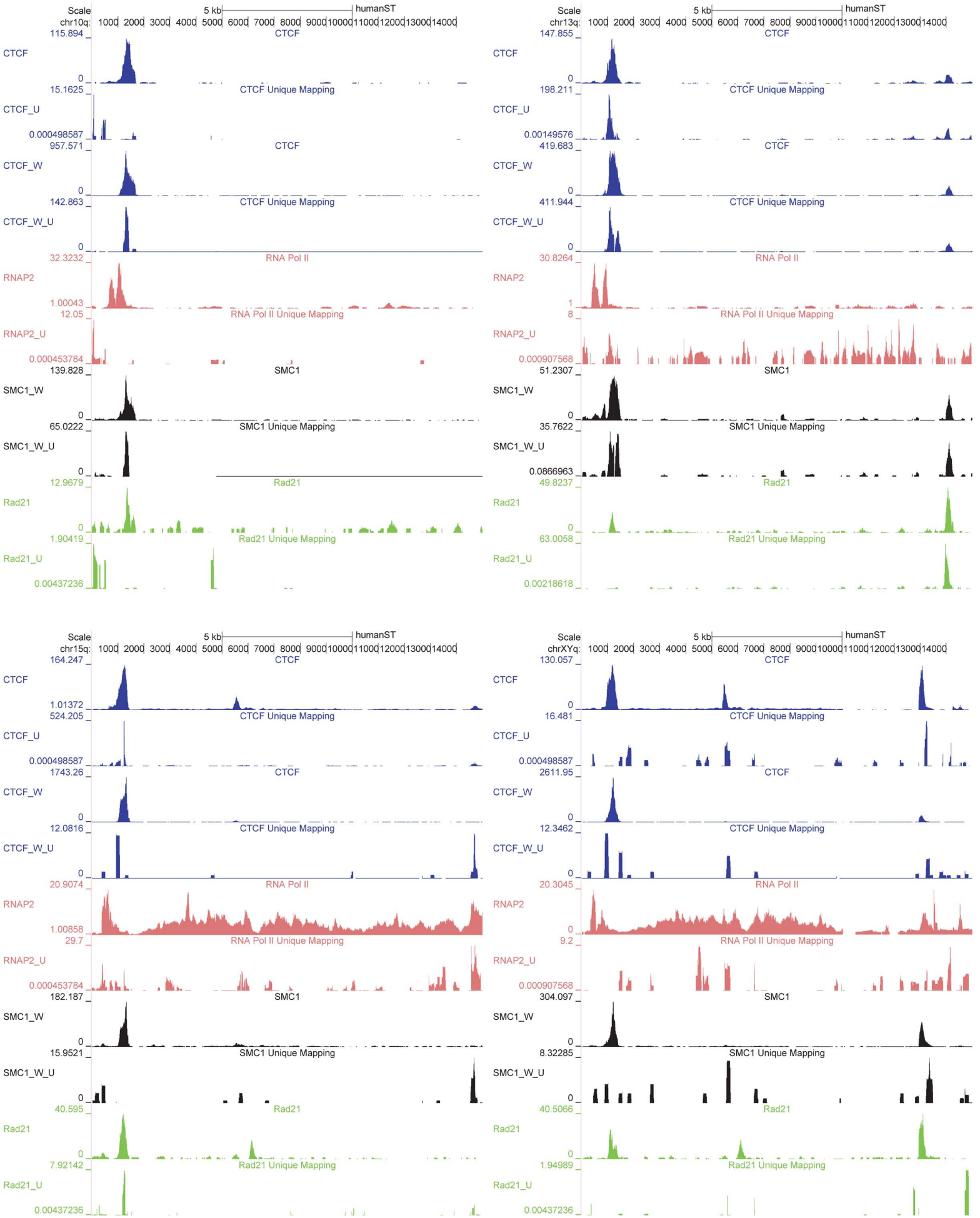
Scale
chr10q:
5 kb
humanST
1000 2000 3000 4000 5000 6000 7000 8000 9000 10000 11000 12000 13000 14000
115.894
CTCF
CTCF
0
15.1625
CTCF Unique Mapping
CTCF_U
0.000498587
957.571
CTCF
CTCF_W
0
142.863
CTCF Unique Mapping
CTCF_W_U
0
32.3232
RNA Pol II
RNAP2
1.00043
12.05
RNA Pol II Unique Mapping
RNAP2_U
0.000453784
139.828
SMC1
SMC1_W
0
65.0222
SMC1 Unique Mapping
SMC1_W_U
0
12.9679
Rad21
Rad21
0
1.90419
Rad21 Unique Mapping
Rad21_U
0.00437236
Scale
chr13q:
5 kb
humanST
1000 2000 3000 4000 5000 6000 7000 8000 9000 10000 11000 12000 13000 14000
147.855
CTCF
CTCF
0
198.211
CTCF Unique Mapping
CTCF_U
0.00149576
419.683
CTCF
CTCF_W
0
411.944
CTCF Unique Mapping
CTCF_W_U
0
30.8264
RNA Pol II
RNAP2
1
8
RNA Pol II Unique Mapping
RNAP2_U
0.000907568
51.2307
SMC1
SMC1_W
0
35.7622
SMC1 Unique Mapping
SMC1_W_U
0.0866963
49.8237
Rad21
Rad21
0
63.0058
Rad21 Unique Mapping
Rad21_U
0.00218618
Scale
chr15q:
5 kb
humanST
1000 2000 3000 4000 5000 6000 7000 8000 9000 10000 11000 12000 13000 14000
164.247
CTCF
CTCF
1.01372
524.205
CTCF Unique Mapping
CTCF_U
0.000498587
1743.26
CTCF
CTCF_W
0
12.0816
CTCF Unique Mapping
CTCF_W_U
0
20.9074
RNA Pol II
RNAP2
1.00858
29.7
RNA Pol II Unique Mapping
RNAP2_U
0.000453784
182.187
SMC1
SMC1_W
0
15.9521
SMC1 Unique Mapping
SMC1_W_U
0
40.595
Rad21
Rad21
0
7.92142
Rad21 Unique Mapping
Rad21_U
0.00437236
Scale
chrXYq:
5 kb
humanST
1000 2000 3000 4000 5000 6000 7000 8000 9000 10000 11000 12000 13000 14000
130.057
CTCF
CTCF
0
16.481
CTCF Unique Mapping
CTCF_U
0.000498587
2611.95
CTCF
CTCF_W
0
12.3462
CTCF Unique Mapping
CTCF_W_U
0
20.3045
RNA Pol II
RNAP2
0
9.2
RNA Pol II Unique Mapping
RNAP2_U
0.000907568
304.097
SMC1
SMC1_W
0
8.32285
SMC1 Unique Mapping
SMC1_W_U
0
40.5066
Rad21
Rad21
0
1.94989
Rad21 Unique Mapping
Rad21_U
0.00437236

Fig. S2

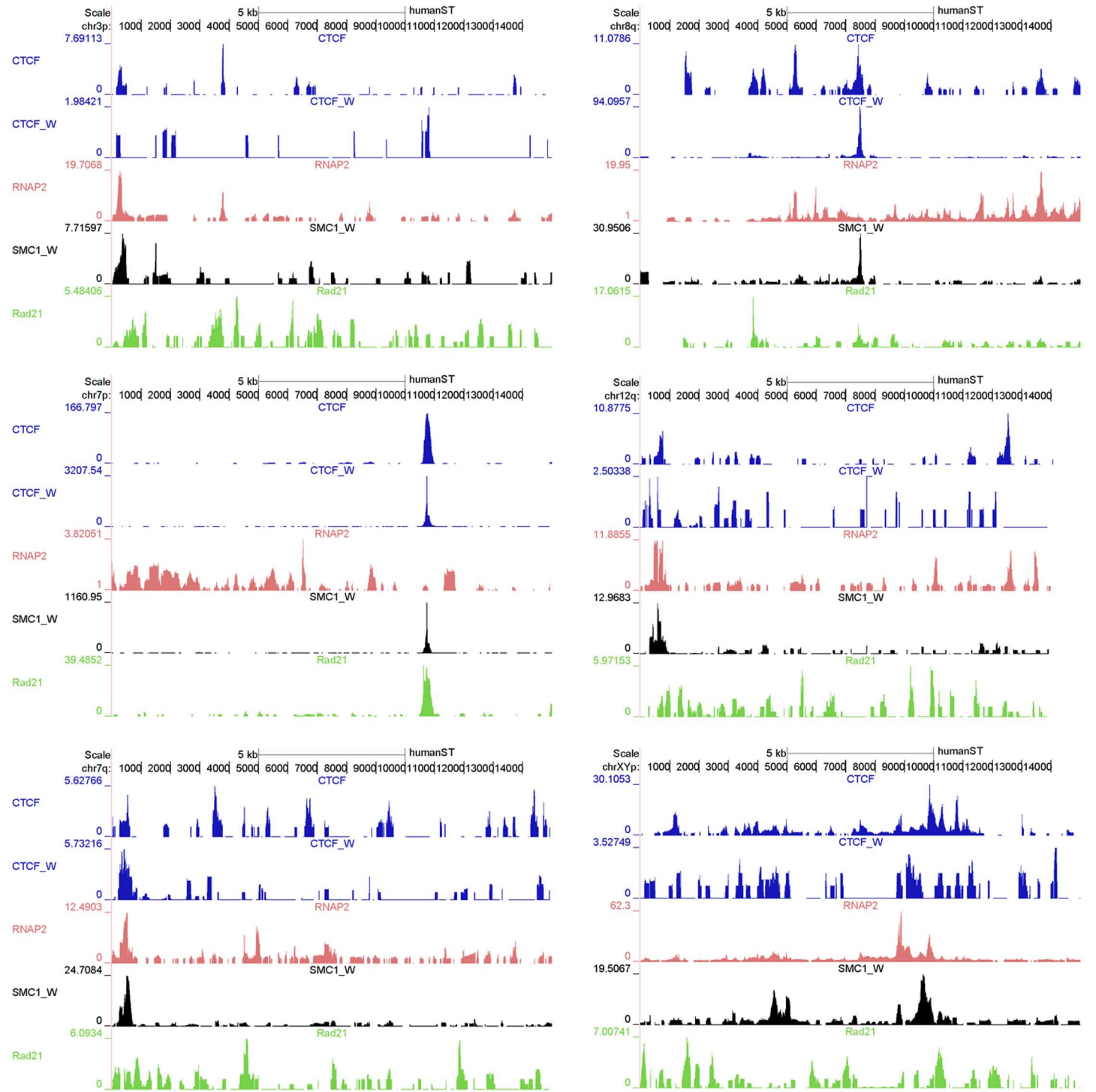
Scale
5 kb
humanST
chr3p:
chr8q:
chr7p:
chr12q:
chr7q:
chrXYp:
CTCF
CTCF_W
RNAP2
SMC1_W
Rad21

Fig. S3

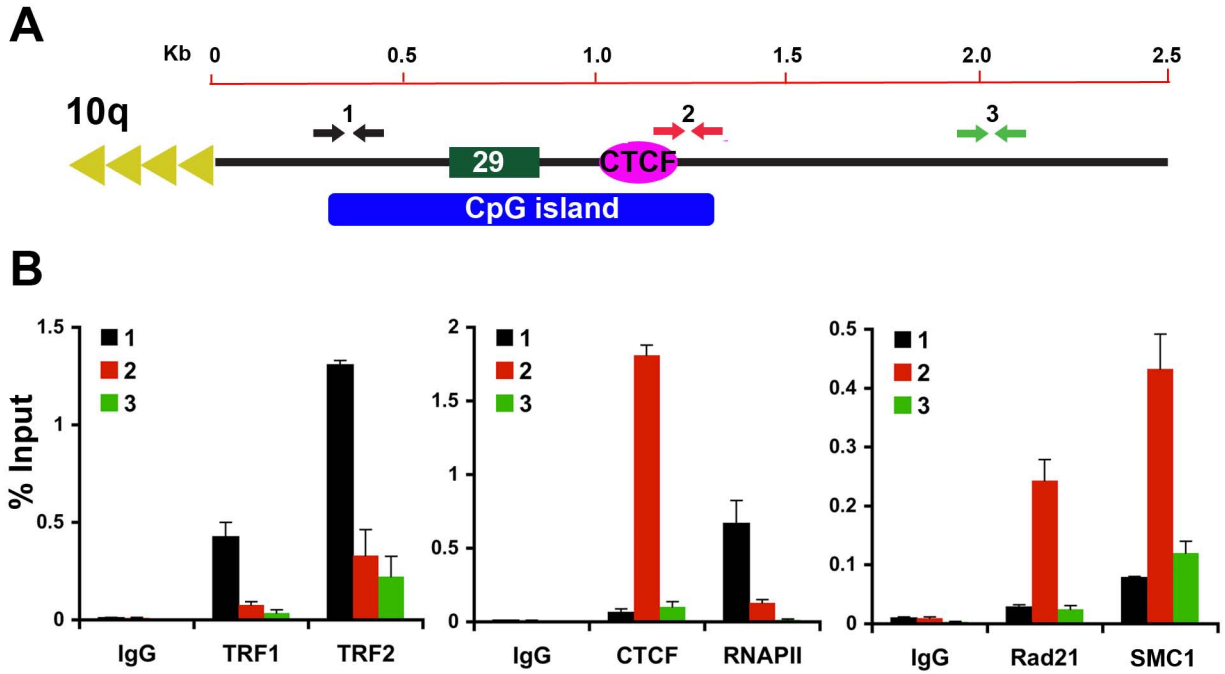
A
Kb
0
0.5
1.0
1.5
2.0
2.5
10q
1
2
3
29
CTCF
CpG island
B
% Input
1
2
3
IgG
TRF1
TRF2
IgG
CTCF
RNAPII
IgG
Rad21
SMC1

Fig. S4

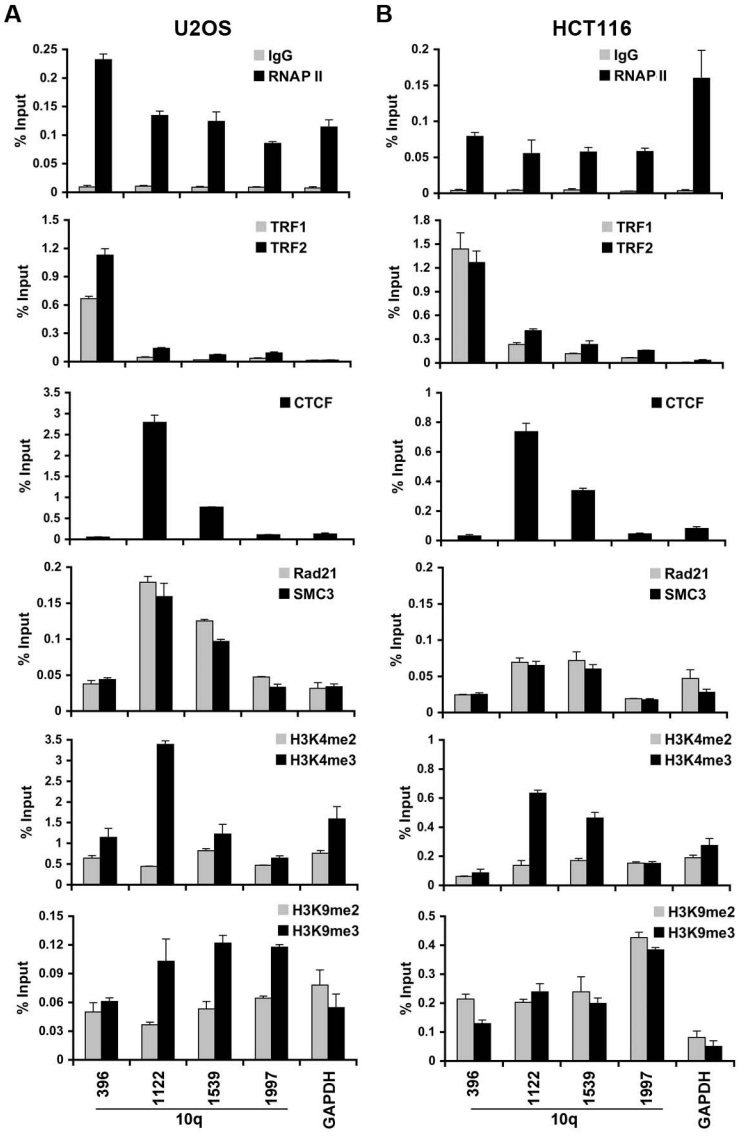
A
U2OS
B
HCT116
IgG
RNAP II
TRF1
TRF2
CTCF
Rad21
SMC3
H3K4me2
H3K4me3
H3K9me2
H3K9me3
% Input
396
1122
1539
1997
GAPDH
10q

Fig. S5

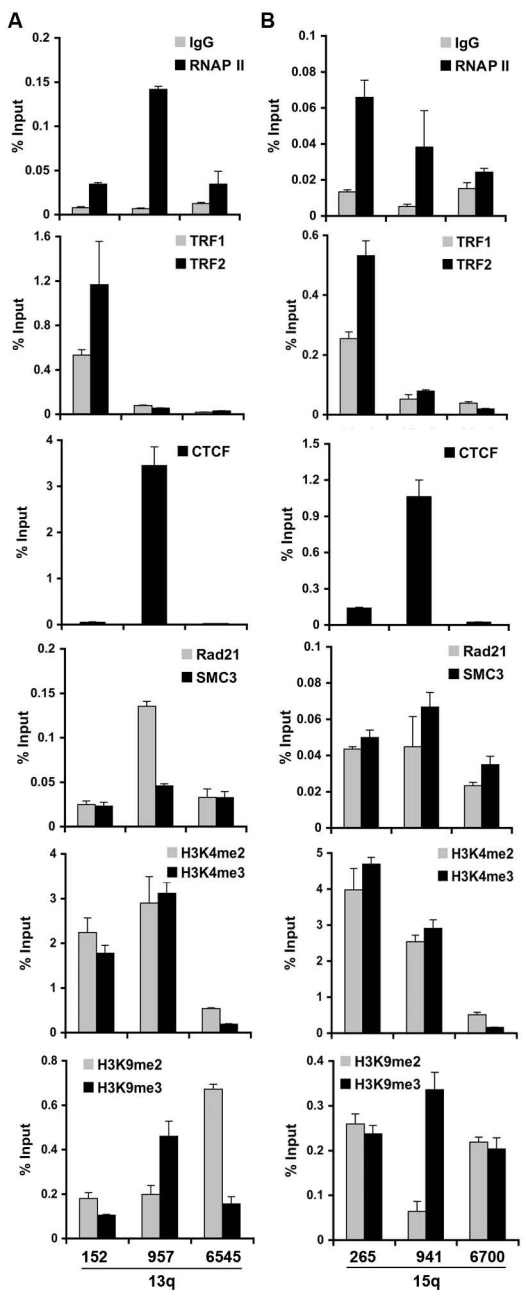
A
B
IgG
RNAP II
% Input
TRF1
TRF2
CTCF
Rad21
SMC3
H3K4me2
H3K4me3
H3K9me2
H3K9me3
152
957
6545
13q
265
941
6700
15q

Fig. S6

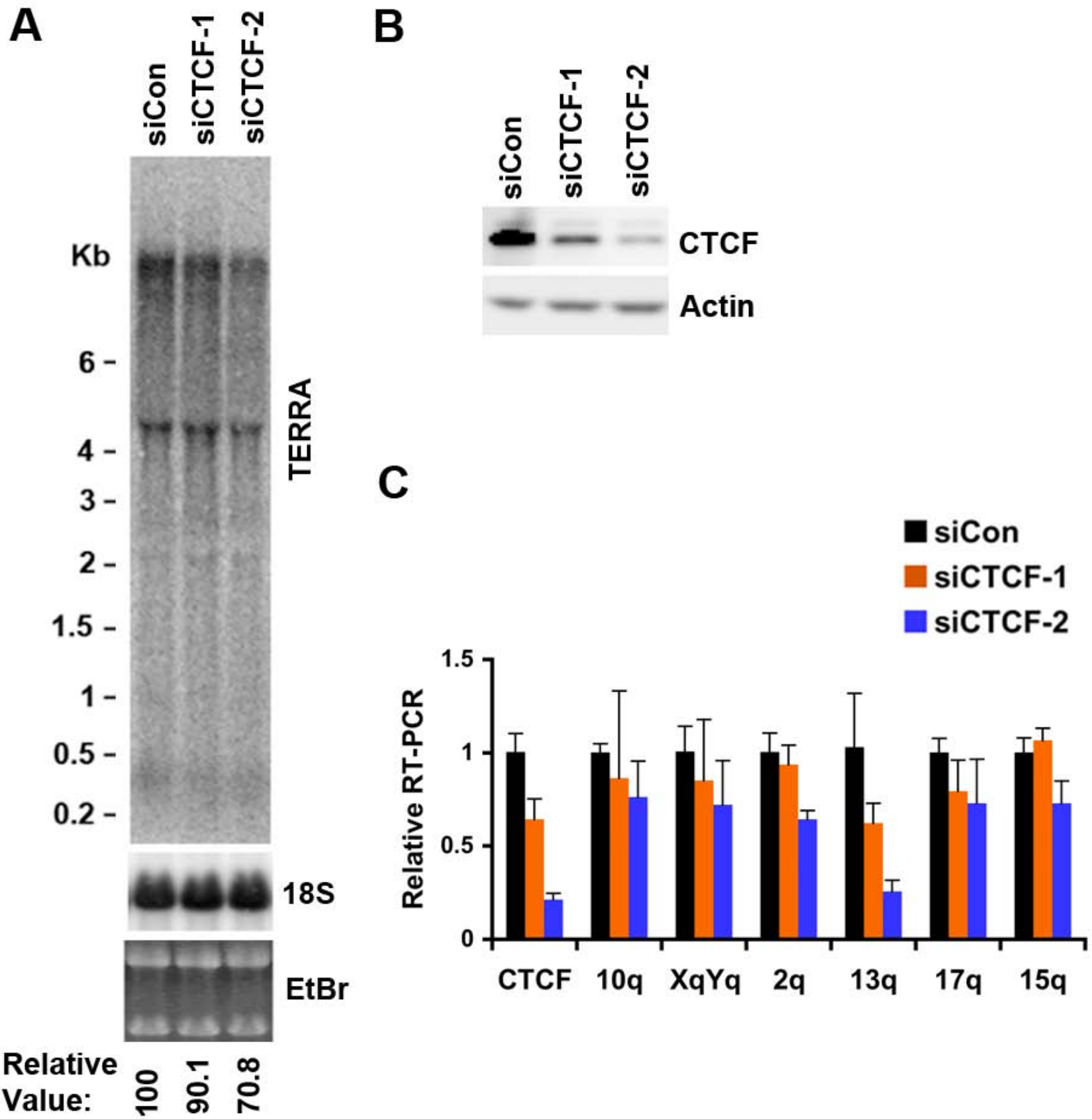
A
siCon
siCTCF-1
siCTCF-2
Kb
6
4
3
2
1.5
1
0.5
0.2
TERRA
18S
EtBr
Relative Value:
100
90.1
70.8
B
siCon
siCTCF-1
siCTCF-2
CTCF
Actin
C
siCon
siCTCF-1
siCTCF-2
Relative RT-PCR
1.5
1
0.5
0
CTCF
10q
XqYq
2q
13q
17q
15q

Fig. S7

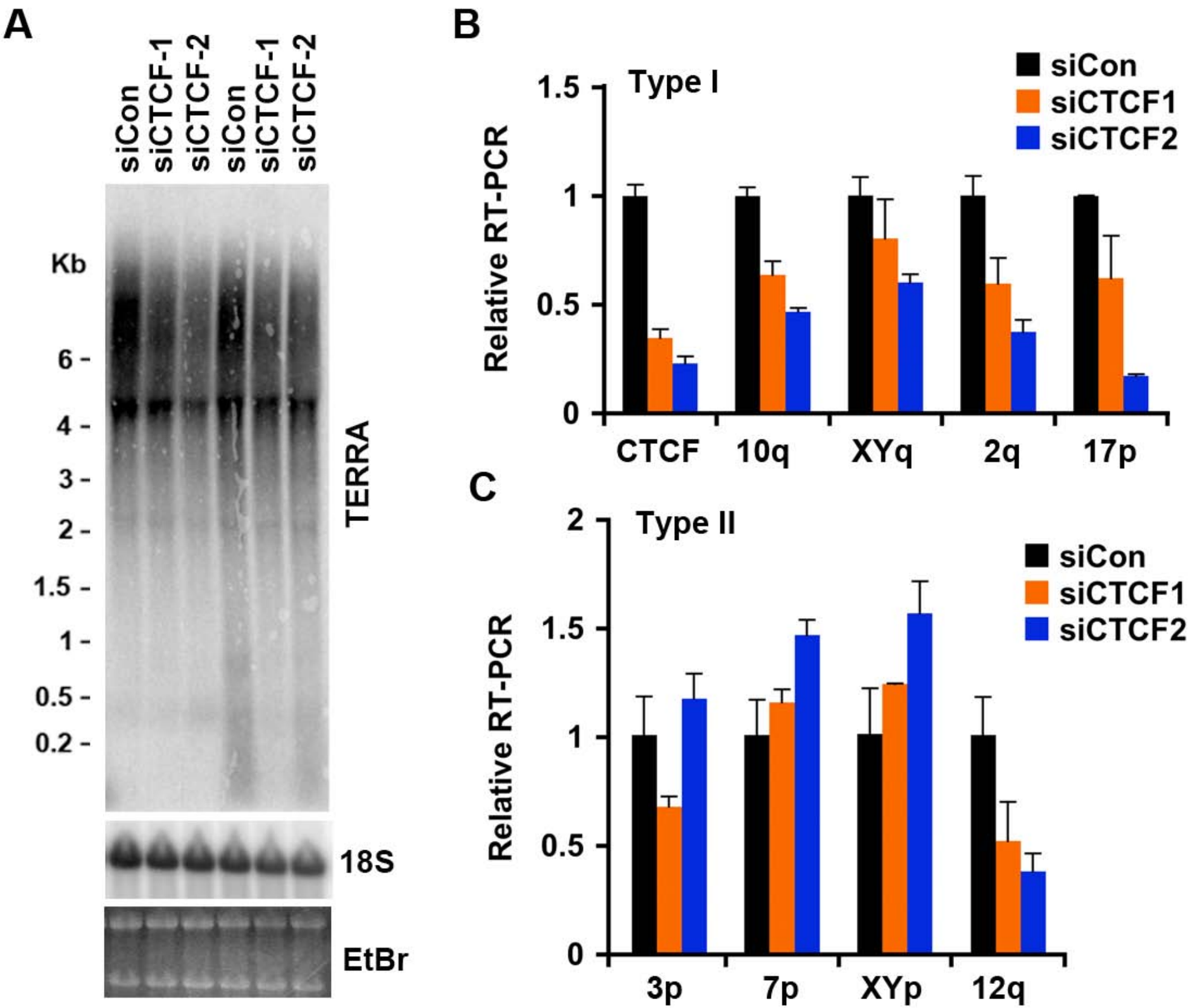
A
siCon
siCTCF-1
siCTCF-2
siCon
siCTCF-1
siCTCF-2
Kb
6
4
3
2
1.5
1
0.5
0.2
TERRA
18S
EtBr
B
Type I
siCon
siCTCF1
siCTCF2
Relative RT-PCR
1.5
1
0.5
0
CTCF
10q
XYq
2q
17p
C
Type II
siCon
siCTCF1
siCTCF2
Relative RT-PCR
2
1.5
1
0.5
0
3p
7p
XYp
12q

Fig. S8

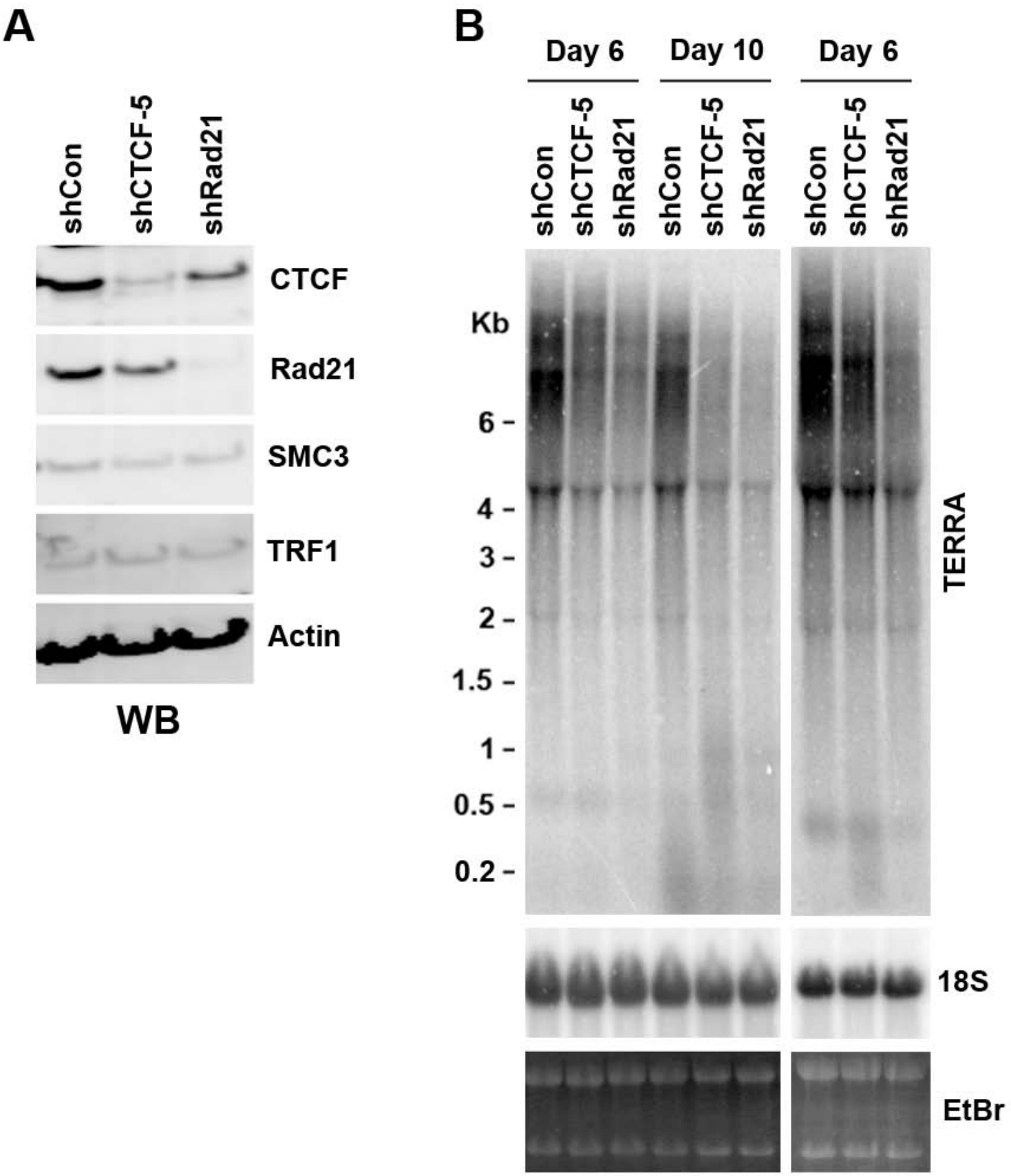
A
shCon
shCTCF-5
shRad21
CTCF
Rad21
SMC3
TRF1
Actin
WB
B
Day 6
Day 10
Day 6
shCon
shCTCF-5
shRad21
shCon
shCTCF-5
shRad21
shCon
shCTCF-5
shRad21
Kb
6
4
3
2
1.5
1
0.5
0.2
TERRA
18S
EtBr

Fig. S9

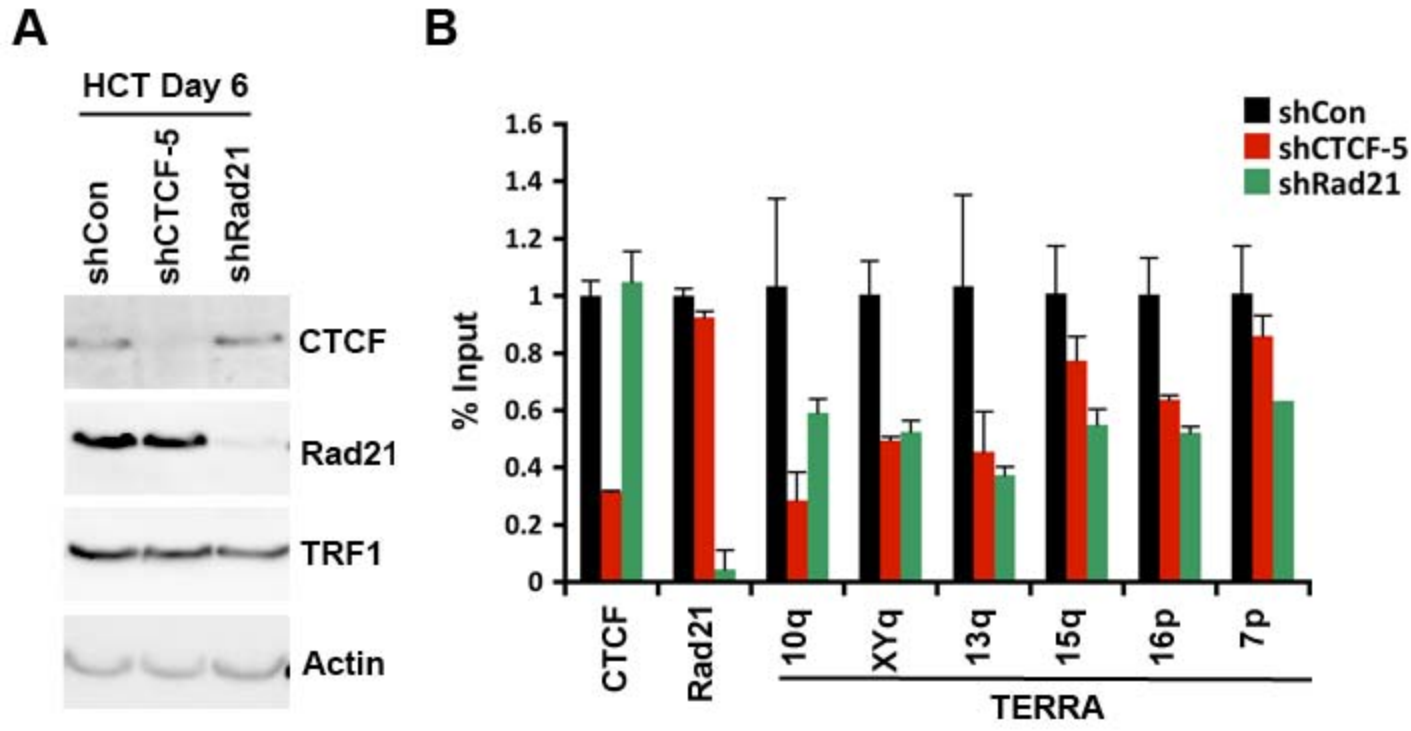
A
HCT Day 6
shCon
shCTCF-5
shRad21
CTCF
Rad21
TRF1
Actin
B
shCon
shCTCF-5
shRad21
% Input
1.6
1.4
1.2
1
0.8
0.6
0.4
0.2
0
CTCF
Rad21
10q
XYq
13q
15q
16p
7p
TERRA

Fig. S10

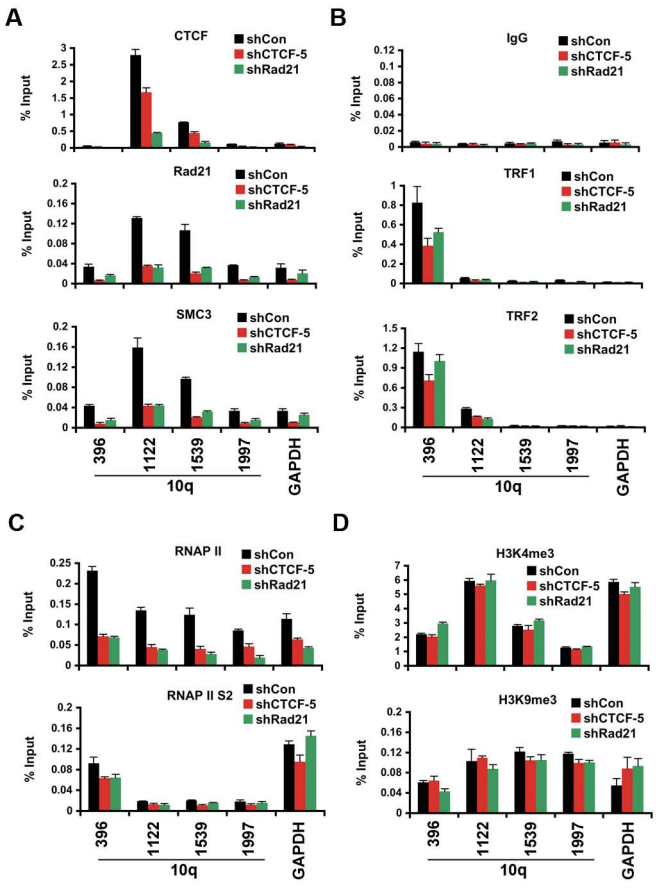
A
CTCF
shCon
shCTCF-5
shRad21
% Input
Rad21
SMC3
B
IgG
TRF1
TRF2
396
1122
1539
1997
GAPDH
10q
C
RNAP II
RNAP II S2
D
H3K4me3
H3K9me3

Fig. S11

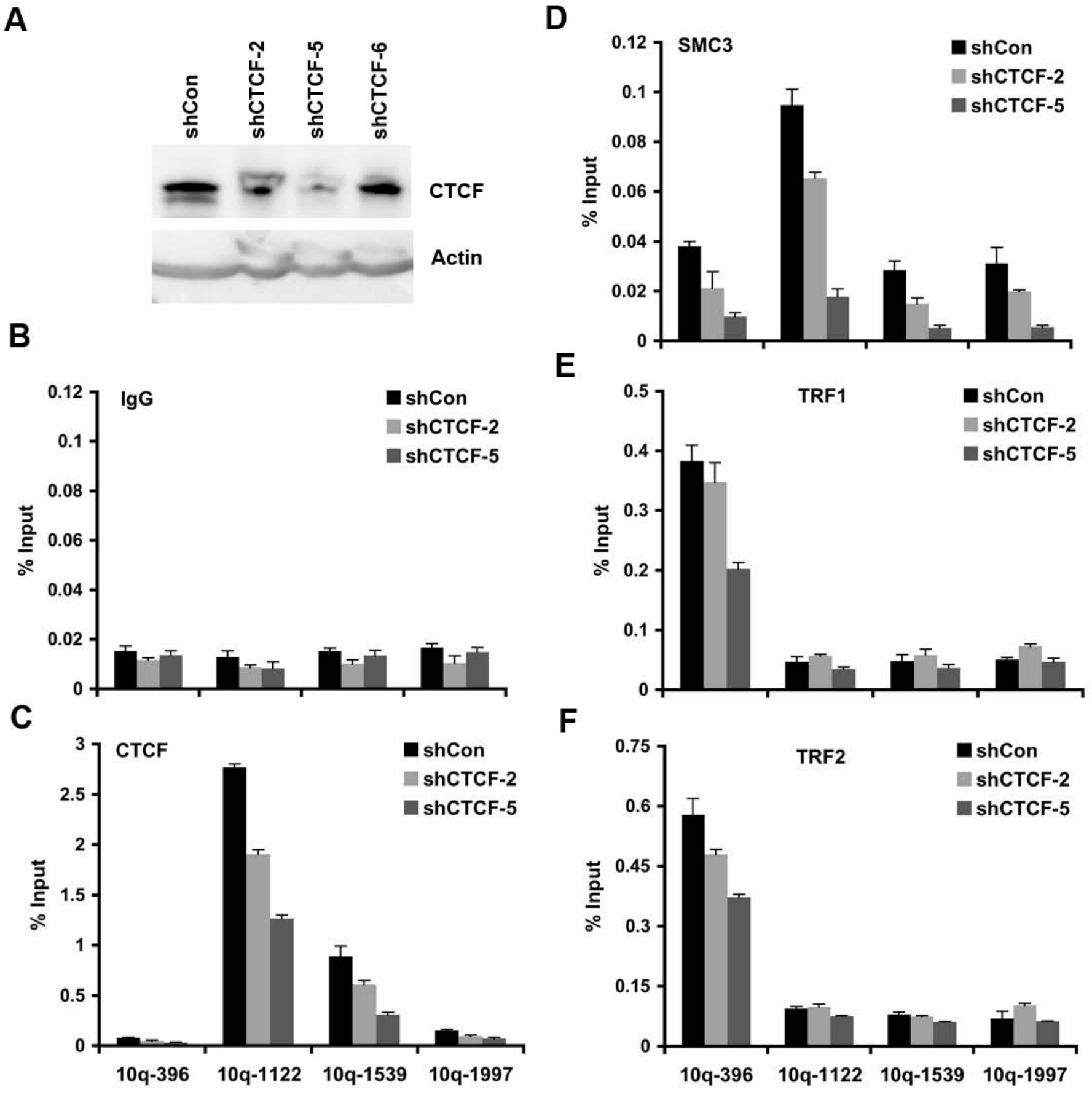
A
shCon
shCTCF-2
shCTCF-5
shCTCF-6
CTCF
Actin
B
IgG
shCon
shCTCF-2
shCTCF-5
% Input
0.12
0.1
0.08
0.06
0.04
0.02
0
C
CTCF
shCon
shCTCF-2
shCTCF-5
% Input
3
2.5
2
1.5
1
0.5
0
10q-396
10q-1122
10q-1539
10q-1997
D
SMC3
shCon
shCTCF-2
shCTCF-5
% Input
0.12
0.1
0.08
0.06
0.04
0.02
0
E
TRF1
shCon
shCTCF-2
shCTCF-5
% Input
0.5
0.4
0.3
0.2
0.1
0
F
TRF2
shCon
shCTCF-2
shCTCF-5
% Input
0.75
0.6
0.45
0.3
0.15
0
10q-396
10q-1122
10q-1539
10q-1997

Fig. S12

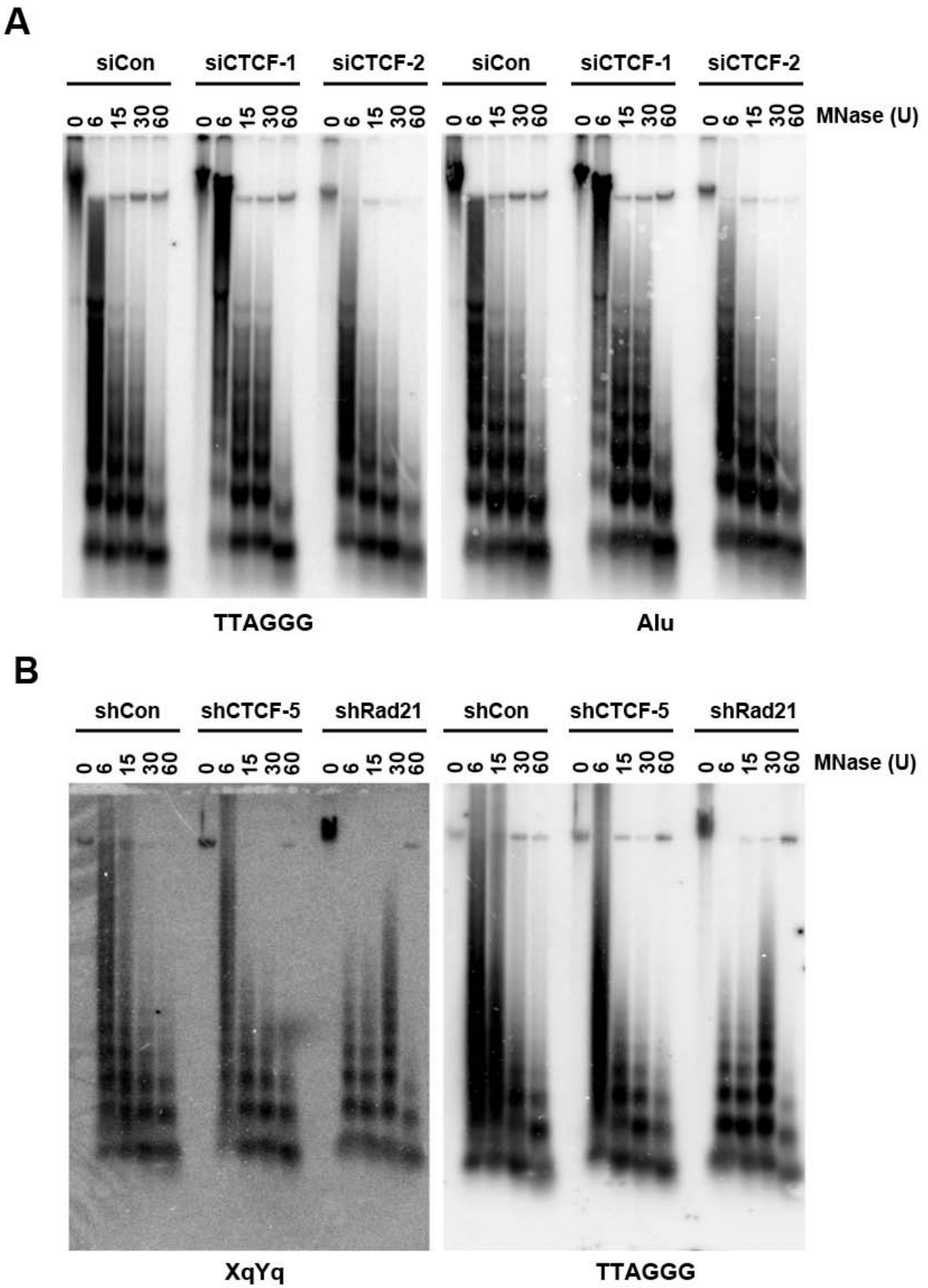
A
siCon
siCTCF-1
siCTCF-2
siCon
siCTCF-1
siCTCF-2
0 6 15 30 60
MNase (U)
TTAGGG
Alu
B
shCon
shCTCF-5
shRad21
shCon
shCTCF-5
shRad21
0 6 15 30 60
MNase (U)
XqYq
TTAGGG

Fig. S13

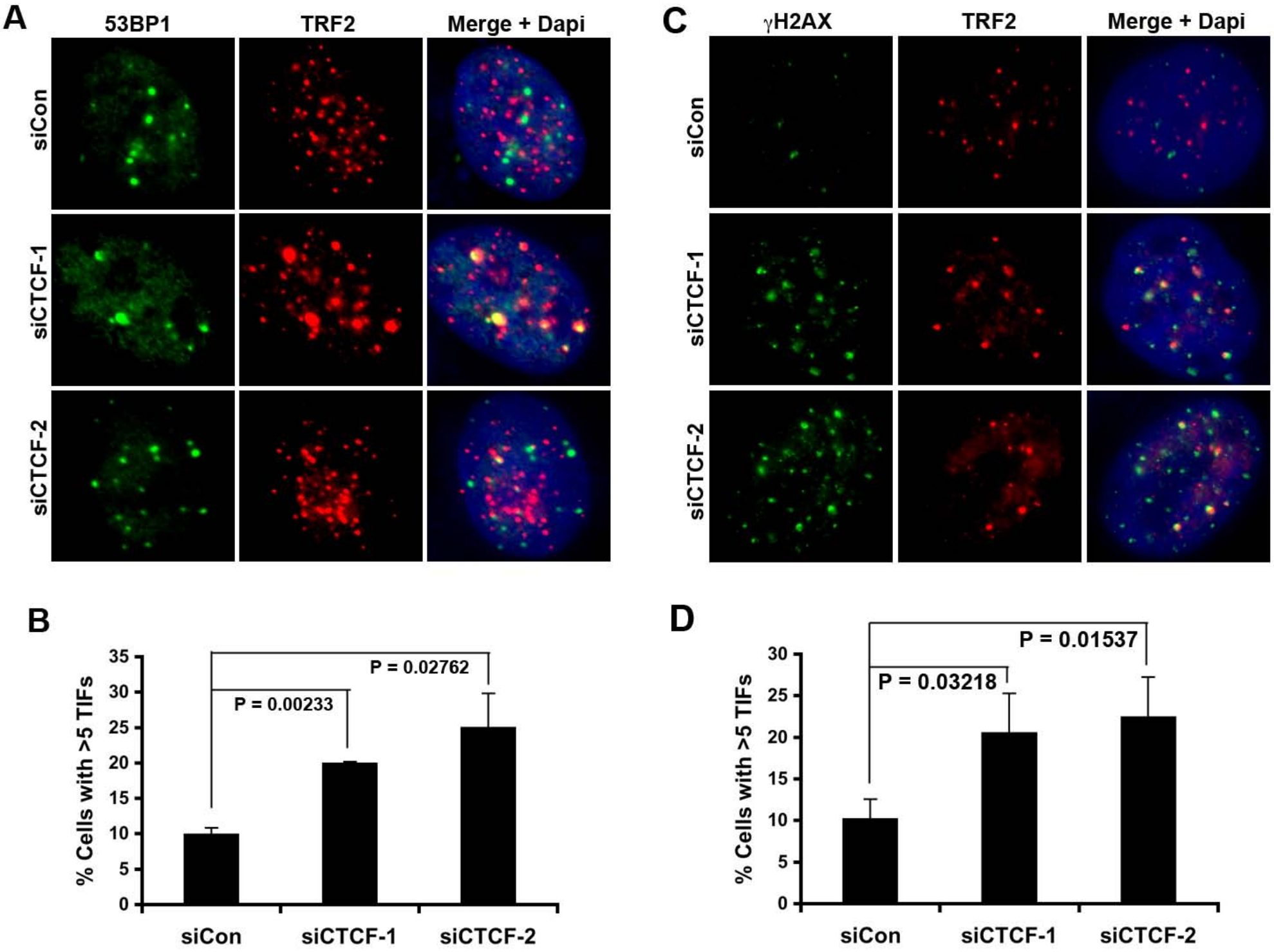
A
53BP1
TRF2
Merge + Dapi
siCon
siCTCF-1
siCTCF-2
C
γH2AX
TRF2
Merge + Dapi
siCon
siCTCF-1
siCTCF-2
B
% Cells with >5 TIFs
35
30
25
20
15
10
5
0
P = 0.02762
P = 0.00233
siCon
siCTCF-1
siCTCF-2
D
% Cells with >5 TIFs
30
25
20
15
10
5
0
P = 0.01537
P = 0.03218
siCon
siCTCF-1
siCTCF-2

Fig. S14

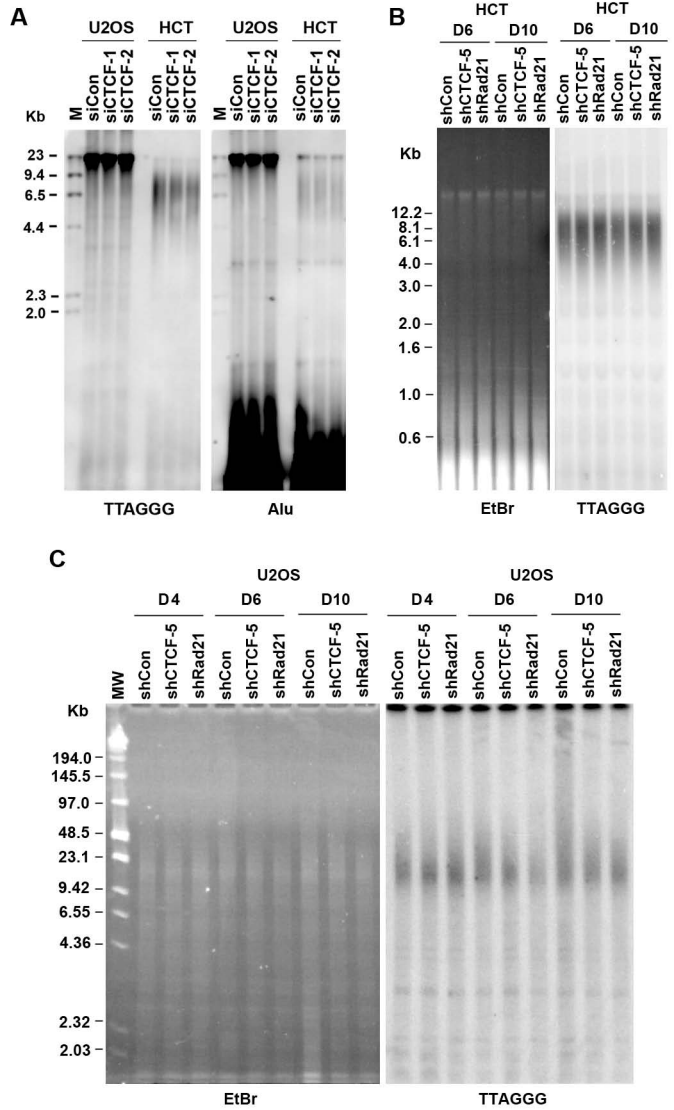
A
U2OS
HCT
U2OS
HCT
M
siCon
siCTCF-1
siCTCF-2
siCon
siCTCF-1
siCTCF-2
M
siCon
siCTCF-1
siCTCF-2
siCon
siCTCF-1
siCTCF-2
Kb
23
9.4
6.5
4.4
2.3
2.0
TTAGGG
Alu
B
HCT
HCT
D6
D10
D6
D10
shCon
shCTCF-5
shRad21
shCon
shCTCF-5
shRad21
shCon
shCTCF-5
shRad21
shCon
shCTCF-5
shRad21
Kb
12.2
8.1
6.1
4.0
3.0
2.0
1.6
1.0
0.6
EtBr
TTAGGG
C
U2OS
U2OS
D4
D6
D10
D4
D6
D10
MW
shCon
shCTCF-5
shRad21
shCon
shCTCF-5
shRad21
shCon
shCTCF-5
shRad21
shCon
shCTCF-5
shRad21
shCon
shCTCF-5
shRad21
shCon
shCTCF-5
shRad21
Kb
194.0
145.5
97.0
48.5
23.1
9.42
6.55
4.36
2.32
2.03
EtBr
TTAGGG

Fig. S15

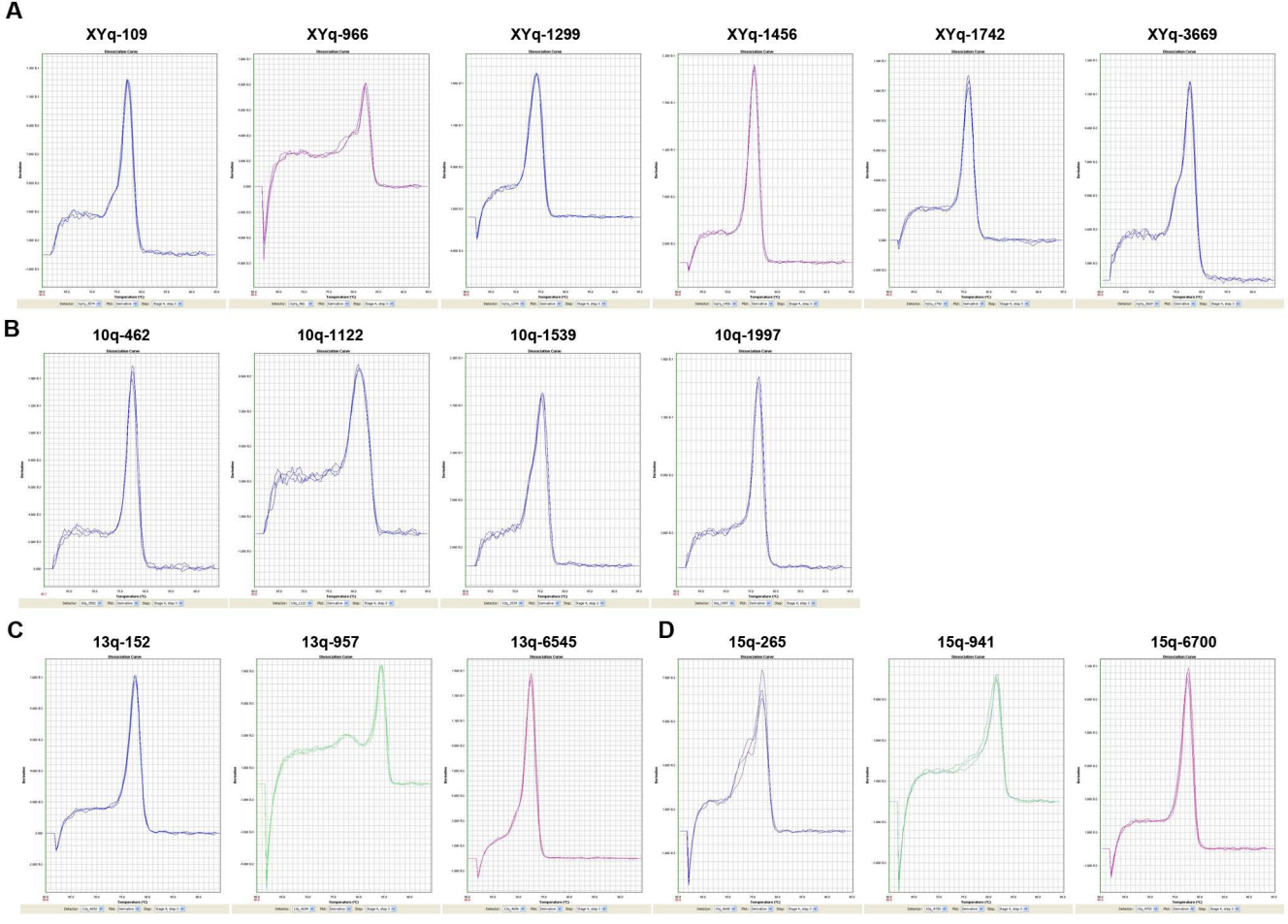
A
XYq-109
XYq-966
XYq-1299
XYq-1456
XYq-1742
XYq-3669
B
10q-462
10q-1122
10q-1539
10q-1997
C
13q-152
13q-957
13q-6545
D
15q-265
15q-941
15q-6700

Fig. S16